ENSTA Bretagne
Ifremer
15ÈMES JOURNÉES DE L'HYDRODYNAMIQUE
22 - 24 novembre 2016 - Brest

Essais en bassin et simulations couplées pour une TLP à lignes inclinées

Model tests and coupled simulations for an inclined-leg TLP

Bozonnet, P.[1], Caillé, F.[2], Melis, C.[2], Poirette, Y.[1], Perdrizet, T.[1]
[1]IFP Energies nouvelles – Etablissement de Lyon
[2] SBM Offshore - Monaco

Résumé

Une nouvelle fondation flottante, de type TLP à lignes inclinées pour éolienne multi-MW est développée par l'alliance IFPEN/SBM Offshore. Une campagne d'essais en bassin a été réalisée en 2015 dans le bassin offshore de MARIN, à l'échelle 1/40ème via la similitude de Froude. L'éolienne MARIN Stock Wind Turbine (MSWT), reproduisant les performances de la NREL 5MW, et le système de génération de vent conçus par MARIN sont utilisés. La campagne d'essais a permis de valider le concept. Ce papier présente la confrontation des données expérimentales aux modèles numériques. Une méthodologie pas à pas permet de valider les aspects structurels et hydrodynamiques. Les méthodes de calibration des coefficients hydrodynamiques semblent également appropriées. Les performances aérodynamiques sont validées, mais certaines différences persistent dans le contenu spectral probablement dues aux spécificités du vent et de la structure de la MSWT. Les simulations avec un couplage aérodynamique simplifié montrent un bon accord avec les données expérimentales. Le travail de simulation avec un calcul direct de l'aérodynamique via un modèle BEM reste à réaliser pour valider l'ensemble de la chaîne de calcul.

Summary

From a collaboration between SBM Offshore and IFPEN, a new concept for Floating Wind Turbine (FWT) is proposed: an inclined-leg TLP. A model test campaign has been performed in 2015, in MARIN's offshore basin, at scale 1/40 (Froude similitude). The MARIN Stock Wind Turbine (MSWT), able to mimic the NREL 5MW performances, as well as the wind generator designed specifically for FWT were provided by MARIN. The model tests validated the innovative concepts. This paper focuses on the numerical models and tools validation. A step-by-step methodology allows for a hydrodynamics and structural properties check. The hydrodynamic coefficient methodology is validated at model-scale and thus will be extrapolated at full-scale. The aerodynamic performances of the MSWT and the numerical model are validated thanks to onshore tests, accounting for the basin specificities is also crucial. Simplified coupled simulations show a good agreement with the experimental data, and fully coupled simulations with aerodynamic efforts computed thanks to the BEM theory are the next step towards complete validation of the numerical tools.

1. Introduction

A new floating foundation for wind turbine, made up of 4 buoys (3 side buoys and one central buoy) connected by a brace structure, is jointly developed by SBM Offshore and IFPEN. The solution is self-installable, meaning the floater can be towed with the turbine already installed on it, thanks to the buoyancy brought by the side buoys piercing the mean sea level (left side of Figure 1-1). For operation the mooring legs are installed and tensioned. They are slightly inclined to limit the floater motion both in production and parked cases, particularly at the nacelle level. In this configuration the buoys are located far below the free surface, which makes the floater transparent to the waves thus limiting the motion and the leg tension. The solution lightness, modularity and self-instability also contribute to reduce the construction, launching, towing and maintenance costs. Details about the behavior of the support and additional information can be found in [1] and [2].

a)  b) 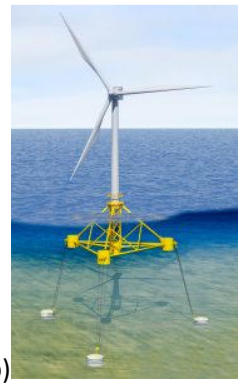

Figure 1-1: Artist views of the concept in a) towing and b) operational configurations

Model test campaign is a necessary step towards a commercial unit: it validates and ensures the proper behavior of the concept. It is also a way to validate the simulation tools used for design, such as Orcaflex (used by SBM Offshore), DeepLinesWind [3] (used by IFPEN) or the CFD software StarCCM. In this respect, model tests have been performed at the Maritime Research Institute Netherlands (MARIN), during three weeks in 2015. The floater design for the 5 MW NREL wind turbine [4] was used since this specific wind turbine is available at scale 1/50 at MARIN. Analysis and simulation work is realized since then.

The present paper aims at presenting this model test campaign, as well as the methodology involved to run representative experiments with simultaneous wave and wind forcing. The simulation tools and strategies will be described, before showing comparisons between simulations and experimental data. A two-step methodology is followed to perform the comparison: the various components of the numerical model are first validated against experimental data from simple tests such as tests with wind turbine only, fixed floater, decay tests, wave or wind only. Secondly, the experimental results with simultaneous wind and waves loads will be discussed and compared to simulations.

2. Model test campaign and methodology

To validate the concept, one would like to simultaneously reproduce at model scale the hydrodynamic and aerodynamic forcing, as well as the structural behavior and the operational performance of the wind turbine. Under correct loadings, one will verify that motion and acceleration at the nacelle remain in the expected range. The structural modes and rotational conditions reproduction is also necessary to check that no undesired and unexpected effects occur in the tensioned system.

The tests were realized in MARIN offshore basin, where wave and current can be generated according to the Froude law similitude. The whole system is scaled down according to this law to properly reproduce the behavior of the floating body on waves. However Froude's similitude does not maintain the Reynolds number since the cinematic viscosity v of air and water is not modified between the model and the full scale device. As a consequence, the aerodynamic forces, as well as the drag forces in water, are not properly scaled down. If geometry is simply scaled-down, the structural properties are not maintained neither.

It is extremely difficult, if not impossible, to match the entire model-scale structural properties of the assembly with the real-scale ones. Therefore, only the tower + Rotor Nacelle Assembly (RNA) (without the floater)

natural resonant frequency is matched with the full scale. The floater structure is made infinitely rigid, and the line axial stiffness has been carefully specified around the pretension (EA = 4.4e6 MN) since it appears to be essential for a correct simulation of the structural modes. Those choices should enable to identify the possible interactions between the wind or the waves and the system structural modes, more especially the mast bending and mooring modes.

On the aerodynamic side, a wind generation system and the Marin Stock Wind Turbine (MSWT) are available at MARIN. As documented in [5], use of low Reynolds blades makes possible "to generate comparable dynamic wind forces as the full scale wind turbine in a Froude-scaled wave and wind environment". Finally it means that the CT-TSR curve is maintained, with:

$$C_T = \frac{T}{\frac{1}{2}\rho U^2 A} \text{ and } TSR = \frac{R\omega}{U}$$

For the present test campaign, the 1/50th scale MSWT has proven to be too heavy. Usually MARIN balances the heavy wind turbine by lightening the floater, taking care that the global mass, inertia and COG are maintained. This is not possible for the TLP because the floater structure is already quite light. As a consequence the campaign as to be performed with a scale factor of 1/40, for which the turbine mass becomes smaller and manageable. Nevertheless, this choice has a significant impact on the aerodynamic forces in the basin, since it modifies the diameter and consequently the rotational speed, the TSR and the thrust as displayed in Table 2-1[1]. At scale 1/40th, one can only decide to maintain the thrust and the TSR (1st set-point) or the thrust and the rotational speed (2nd set-point).

	MSWT 1/50	MSWT 1/40 – 1st set-point	MSWT 1/40 – 2nd set-point
D	126 m	100.8 m	100.8 m
U	11.4 m/s	14.25 m/s	26.06 m/s
RPM	12.1 rpm	18.9 rpm	12.1 rpm
TSR	7	7	2.4
Thrust	720 kN	720 kN	720 kN

Table 2-1: Impact of the scale modification on the aerodynamic quantities

For the model tests, the second set point is chosen. Indeed it enables to maintain the periods associated to the rotational speed (1P, 3P, 6P, 9P) and to check there is no interaction with another natural period of the system or unwanted effects. The drawback of this choice is the low TSR (2.4 instead of 7). This TSR is not within the normal operating range, high angles of attack are at stake (20 to 60°), thus stall or other unexpected aerodynamic phenomena could occur. It has been checked, based on standard deviation, that the thrust variability at this set-point is mainly associated to the inherent variability in the wind (turbulence intensity) and not to stall. The pitch angle is set to 2° in order to get a thrust force exactly equal to 720 kN, the design value.

The final model scale and the setup in the basin are shown on Figure 2-1, main dimensions are summed up in Table 2-2.

Floater draft	26 m	Floater / fairlead radius	45 m
Floater height (keel to mast bottom)	35 m	Turbine and floater mass	1755 t
Hub height (wrt. free surface)	83 m		

Table 2-2: Setup main dimensions at full scale

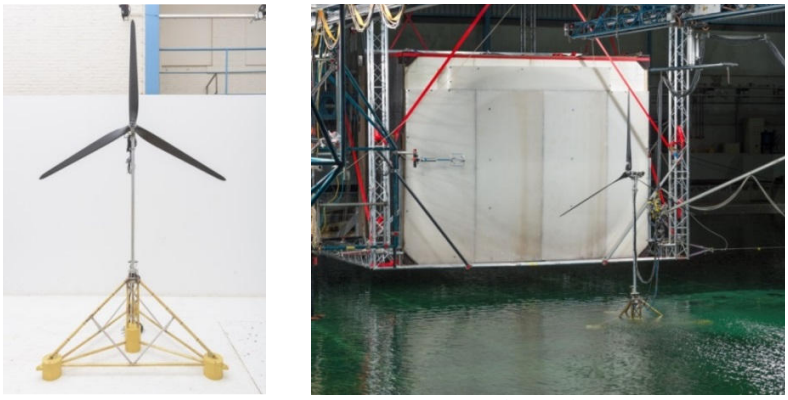

Figure 2-1: Scale model and setup in the basin in front of the wind generation system

[1] All the dimensions and results are given at full scale.

As mentioned in introduction, many tests are performed to enable a step-by-step comparison with simulations and to increase the understanding of the system: fixed (onshore) wind turbine, dip and captive tests, static load tests, hammer tests, current only, wave only, wind only. Finally four extreme sea states and two wind speeds are tested for operational and parked wind turbine in aligned rotor/wind conditions (see Table 2-3), on different configurations such as two water depths (60 and 100 m) or two orientations of the floater, leading to 18 tests in total. During the tests, the response of the floating wind turbine model is recorded through the following measurements: float motion, nacelle acceleration, mooring tensions, tower-top and bottom forces and moments, rotational speed.

	Wave Hs (m)	Wave Tp (s)	Wave direction (°)	Wind speed (m/s)	Current speed (m/s)
Production	6	10 and 14	0 and 30	26	0
Parked	10	14 and 18	0 and 30	45	0 and 0.5

Table 2-3: Extreme environmental conditions for the wind and wave cases

The methodology of the model tests analysis is illustrated on Figure 2-2. The next section will describe the numerical model and the characteristics of the simulations that have been performed (SCS and FCS). The validity of the numerical models is checked in the following sections, first on hydrodynamic and structural aspects, second on aerodynamic aspects. This article only focuses on the Hydro and Aero analyses but does not address the fully coupled simulation stage.

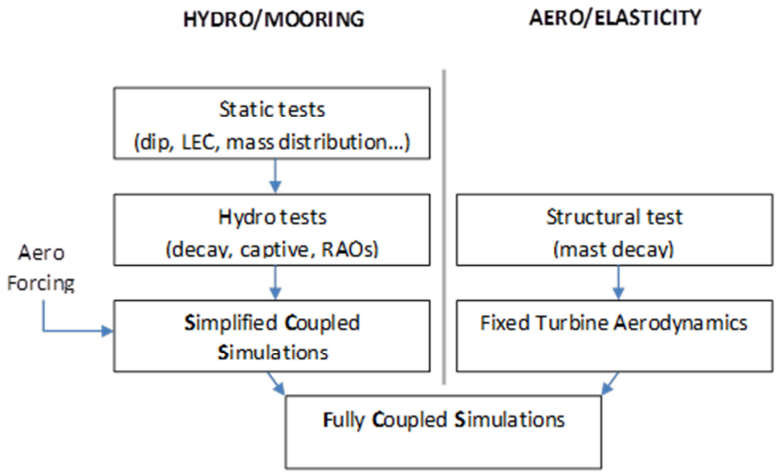

Figure 2-2: Model test analysis methodology

3. Numerical models

Two simulations tools are used, namely Orcaflex (hydro-elastic) and DeepLinesWind (aero-servo-hydro-elastic). Hydrodynamic and structural models are very similar whereas two different approaches are used for aerodynamic and control simulation. In both software, the simulations are performed at full scale but aim, in this paper, at reproducing exactly the model tests.

Given the buoy and bracing dimensions, as well as the relevant sea states, the central and side buoys are simulated with potential flow theory. A single hydrodynamic database is computed with the diffraction – radiation solvers DIODORE or Aqwa since the floater is considered rigid. Morison drag elements are added in the axial direction to take into account the damping due to vortex shedding at the buoy sharp edges and in normal direction for current loads. For bracing hydrodynamic loads, Morison elements are implemented to simultaneously model the wave and current loads.

Drag and inertia coefficients, on the bracing and on the buoys, can be a priori determined based on DNV RP C205 [6], potential flow or CFD simulations, as well as from SBM Offshore and IFPEN REX. Since viscous effects are at

stake, it is critical to consider basin scale. The coefficient effect on motion and tension, the validity of the a priori calibration and the scaling-up to full scale will be discussed in the simulation part. A priori values of the hydrodynamics coefficients and the method used for their estimation are listed in Table 3-1.

Element	Morison coefficient	Value	Method of estimation
Bracing	Normal Cd	1.2	DNV RP C205
	Normal Ca	1	Diff/rad + DNV RP C205
	Axial Cd	0.0	DNV RP C205
	Axial Ca	0.0	DNV RP C205
Buoys	Normal Cd (current)	0.7	CFD
	Axial Cd (vortex shedding)	5.0	SBM/IFPEN REX on CALM buoys

Table 3-1: Initial drag and inertia coefficient used for Morison elements

First order Airy waves associated to Wheeler stretching are used to model the regular and irregular waves, Jonswap spectrum is used for the latter.

Regarding the structural model, mooring, tower and rotor are implemented with finite elements. Properties are set according to the model tests geometry and materials. Regarding the rotor, since the mechanical properties are unknown, they are set to make the blade rigid a priori.

Now to the subject of aerodynamic and controls, two main types of simulations are performed:

- Simply coupled simulations (SCS), with Orcaflex
- Fully coupled simulations (FCS), with DeepLinesWind

In SCS, the aerodynamic forces are not computed but imposed by various means, such as a drag disk or a precomputed tensor, thus making these simulations much faster to run. In the specific case of model tests, forcing with the experimental data is performed in Orcaflex: the 6-component tensor measured at the tower top is imposed at tower top in the numerical model. Beforehand, the measurement is corrected for mass and inertia effects to avoid to consider those effects twice.

In FCS, using DeepLinesWind, the aerodynamic efforts are computed with the Blade Element Momentum (BEM) theory including corrections for secondary aerodynamic effects: Prandtl type hub and tip loss, S. Øye dynamic inflow, skewed model and tower shadow.

The airfoil types and the associated polar curves are considered as suggested in Goupee [7]: two cylinder profiles are used at the blade root, then the MSWT airfoil is used. Goupee computed some initial polar curves that he optimized to reproduce the MSWT measured C_P and C_T curves. The optimization has been made at blade pitch 1° and 15° for a wind speed of 11.4 m/s. The conditions are quite different in the current test campaign: the wind speed is higher (around 25 m/s), the TSR is much lower (around 2.5). The C_P and C_T curves have also been measured, so the same type of comparisons will be performed to ensure the validity of the documented polar plots for the current application.

The wind is implemented thanks to various strategies: the time variation is obtained thanks to standard spectrum such as the Kaimal spectrum or directly from the recorded time variation. Spatial variation is neglected or is generated thanks to TurbSim [8], vertical and horizontal profiles can also be superimposed. Only one constant rotation speed is considered, reached in DeepLinesWind thanks to a PID controller.

The validity of the numerical model described in this paragraph is checked in the coming paragraphs, first on hydrodynamic and structural aspects, second on aerodynamic aspects.

4. Model test and simulation comparison for structural and hydrodynamics validation

This section describes the calibration and checking steps used to validate the adequacy between the numerical model and the basin setup. These steps can be divided into three main categories:

1) Static load: used to validate the mooring arrangement, mass distribution, buoyancy.
2) Structural tests: used to capture the dominant natural modes of the assembly (RNA + Tower + Floater + Lines).
3) Hydrodynamics tests: used to check the hydrodynamics properties of the floater

<u>Static tests</u>

Static tests are mainly used to characterize the geometry, mass and buoyancy repartition of the system. A careful weighting of each element had to be performed in order to match the specified overall assembly mass distribution. A dip test has also insured that the model buoyancy distribution matches the specified one (see dip test results displayed in Figure 4-1).

	Mass[t]	Xcog[m]	Zcog[m]	Ixx[tm2]	Iyy[tm2]	Izz[tm2]
Specified	1753	0.153	30.1	3.42e6	3.40e6	1.27e6
As built	1751	0.128	30.1	3.39e6	3.40e6	1.29e6

Table 4-1: Assembly mass distribution in operational condition, specified vs as-built values

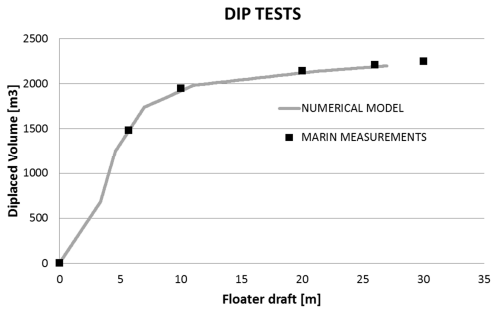

Floater draft [m]	MARIN displaced volume [m3]	MODEL displaced volume [m3]	Relative error [%]
0.0	0.0	0.0	0.0
5.7	1486	1474	0.8
10	1950	1921	1.5
20	2146	2121	1.2
26	2210	2188	1.0
30	2253	2230	1.0

Figure 4-1: Dip test results, MARIN vs numerical model

Static load excursion curves are built experimentally by pulling on the floater and by measuring the corresponding COG displacement and line tensions. The comparison between the experimental and numerical load excursion curves is given on Figure 4-2; one can observe the very good match between the basin as-built system and its numerical model.

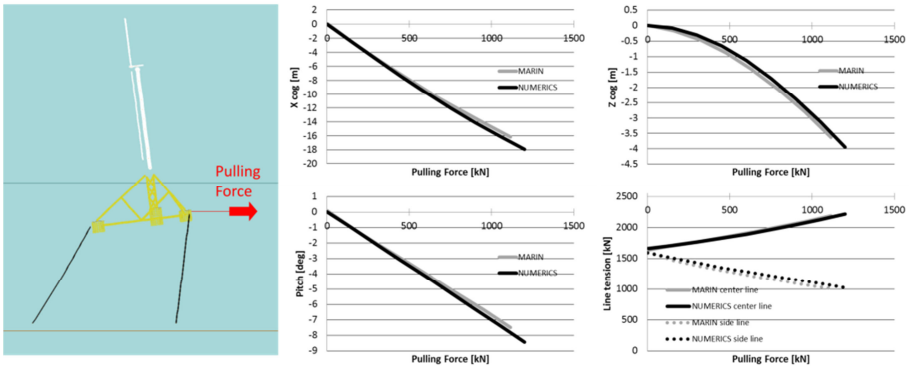

Figure 4-2: Load excursion curves comparison

Structural tests

As said before, tower geometry and material are selected to match the tower + RNA natural resonant frequency. The agreement between model tests and simulation is quite good (Figure 4-3) and lead to a resonant period equal to 2.13 s.

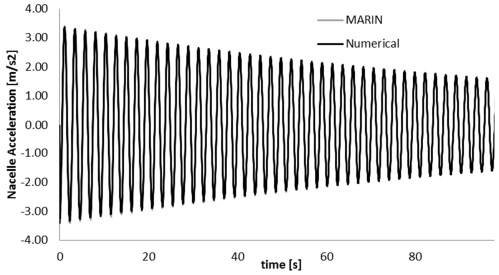

Tower length [m]	66.6
OD [m]	1.68
ID[m]	1.52
Mass per unit length [t/m]	1.231
Bending stiffness [kN.m2]	356e6
Connection Stiffness [kNm/deg]	715e3

Figure 4-3: Tower decay test comparison and as-built characteristics

In order to identify the predominant modes of the assembly, a hammer test has been done by pulling one mooring line and suddenly releasing it. Figure 4-4 shows the mooring line tension spectral density measured in the basin and simulated in ORCAFLEX during this hammer test.

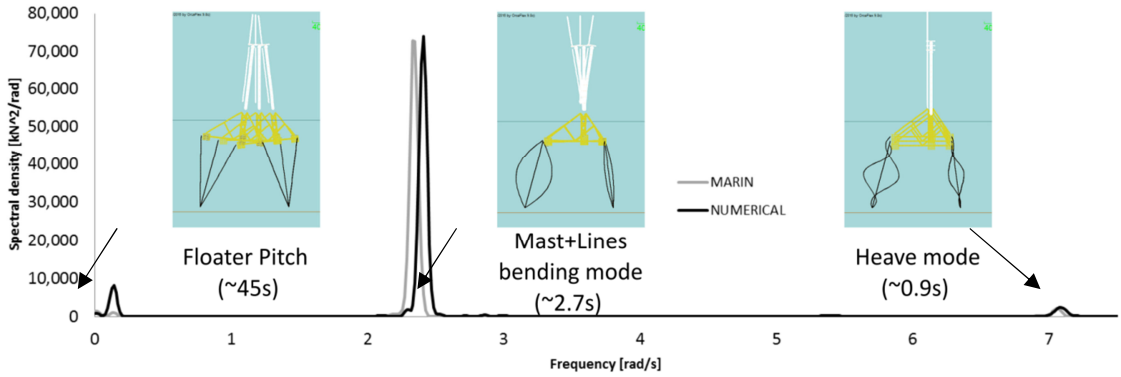

Figure 4-4: Hammer test: mooring line tension spectral density, MARIN vs ORCAFLEX

A fairly good agreement is observed between the measurements and the simulation. On this figure one can observe three dominant modes:

- At approximately 45s, one can identify the floater pitch (or roll) mode (solid body motion).
- The largest peak at 2.7s (slightly underestimated with Orcaflex at 2.6s) corresponds to the tower + mooring lines bending mode (the numerical Rayleigh damping for the tower has been tuned at 0.37% critical to match the amplitude).
- Towards higher frequencies, at 0.9s, is the heave mode.

Hydrodynamics validation

The goal of the hydrodynamics tests is to use simple protocols to assess the coefficients of the numerical model described in paragraph 3. From the hydrodynamics point of view, there are 4 main coefficients:

1) Bracing elements normal added mass coefficient (Can_bracing).
2) Bracing elements normal drag coefficients (Cdn_bracing).
3) Buoys normal drag coefficients (Cdn_buoy).
4) Buoys axial drag coefficients (Cdax_buoy).

In an attempt to validate these coefficients beforehand, captive tests have been carried out. These tests consist in holding the floater (no lines, no turbine) beneath a force frame, at the operational draft. Waves (or current) are generated in the basin, and the resulting forces acting on the floater are measured: wave load Response Amplitude Operators (RAOs) (or current force) can be built.

The normal drag coefficients have been assessed with the help of the current captive tests together with some CFD calculations. A good match is obtained with Cdn_bracing = 1.0 and Cdn_buoy = 0.7. One can notice that these values are in good agreement with the preliminary estimation of Table 3-1.

Figure 4-5 a) shows a comparison of the wave load amplitude RAO in surge obtained with the model tests, the numerical model, the CFD calculations and a diffraction analysis of the floater (buoys + bracing). One can observe that the tests, CFD and diffraction are consistent and that an excellent match is achieved with the numerical model by choosing the following set of coefficients: Can_bracing=1.2, Cdn_bracing = 1.0, Cdn_buoy = 0.7 and Cdax_buoy = 5.0 (reference set). Note that these coefficients are consistent with the first estimation (see Table 3-1).

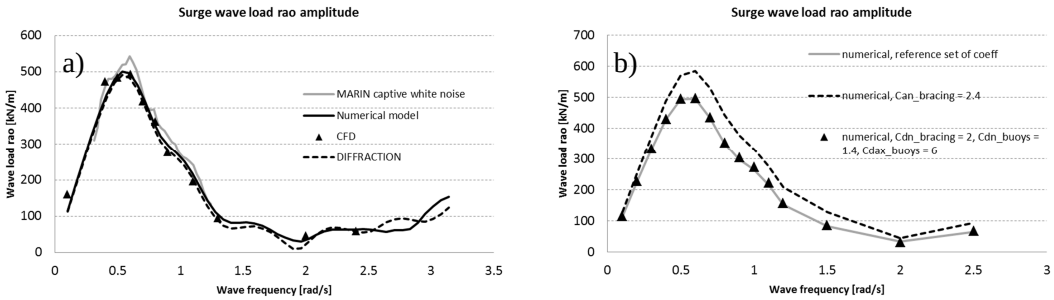

Figure 4-5: Wave load RAO amplitude a): tests, ORCAFLEX, CFD and diffraction comparison b): impact of hydrodynamics coefficients.

On Figure 4-5 b) results from several numerical simulations are plotted, for three sets of hydrodynamics coefficients: doubling the drag coefficient values does not alter the reference curve whereas doubling the bracing added-mass significantly increase the surge wave loads. These results show that the wave loads RAOs are very weakly dependent on the drag coefficients chosen; only the bracing normal added-mass coefficient has a noticeable impact.

Motion RAOs have been measured during the campaign. In this case, the whole system is anchored in the basin (RNA+tower+floater+lines), waves are generated and the corresponding floater motions are measured. Figure 4-6 gives an example of the motion RAO obtained from the measurements and from the numerical simulations for several sets of hydrodynamics coefficients.

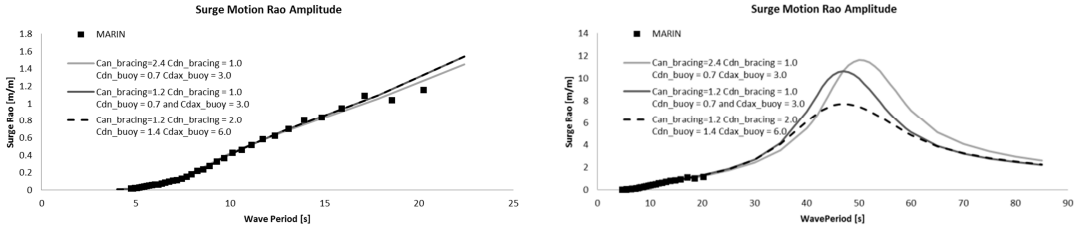

Figure 4-6: Surge motion RAO, influence of hydrodynamics coefficients

In the wave period range (~3s to ~20s), the RAOs are very weakly sensitive to the choice of the hydrodynamics coefficients. They only impact the surge resonant peak: doubling the bracing added-mass coefficient moves the peak period from 45 to 50s, doubling the drag coefficients decreases the peak height of 35%. In the MARIN basin it is not possible to generate waves of periods such that the peak could be captured, consequently it is not possible to select a parameter set rather than another one. For the remaining, the results shown are issued from a numerical model using the reference hydrodynamics data set which lead to the best fit with the captive tests (current and waves): Can_bracing=1.2, Cdn_bracing = 1.0, Cdn_buoy = 0.7 and Cdax_buoy = 5.0.

These results prove that, in the wave frequency range, the system behavior is very weakly impacted by the choice of the drag coefficients (bracing or buoys). The drag only affects the floater motion around the surge resonance, at low frequency. For full scale extrapolation, it is thus reasonable to follow the procedure used during this calibration: the drag coefficients will be estimated through constant current tests simulated by CFD.

The system behavior seems to be more sensitive to the bracing added-mass value. At basin scale, the value obtained seems to be consistent with DNV recommendations: when going to full scale calculations the same DNV recommendation should be used (dependency upon Reynolds and KC number). It could also be envisaged to use CFD calculations in order to estimate its value.

5. Model test and simulation comparison for the fixed wind turbine and aerodynamic validation

To validate the aerodynamic model in DeepLinesWind, tests with a fixed wind turbine are first performed both in parked (no rotation and 90° blade pitch angle) and production mode (rotating turbine). The forces and moments are recorded at tower top and bottom, as well as the acceleration at tower top.

For the simulated parked case, drag forces are considered on the nacelle and along the tower, whose drag coefficients are calibrated to match the measured force at respectively the tower top and tower bottom. The measured wind speed is used directly. Finally a good agreement is obtained on the mean values and standard deviations for tower top acceleration, forces and moments at tower top and bottom. Two resonant peaks appear on the power spectral density as highlighted in Figure 5-1. The first one is the tower first bending mode, the second one is probably due to the blade bending. Thus the blade edge and flap bending stiffness values are, from now on, set to match this peak: EI_{flap} = 4e9 Nm² and EI_{edge} = 7e9 Nm². They are considered constant along the blade.

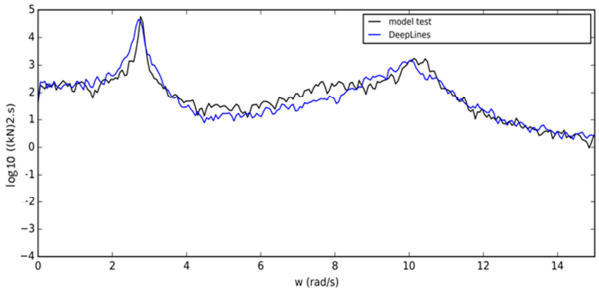

Figure 5-1: Power spectral density of the x-force at tower bottom in the parked case, for the model test (black) and the DeepLinesWind simulation (blue)

Regarding the production case, the experimental and simulated Ct-TSR curves are plotted in Figure 5-2, respectively with markers and lines. The TSR of interest (2.45) leads to a large deviation between model tests and simulation. This is related to the optimization process performed by Goupee [7], focused on TSR values ranging from 3 to 8 with a 1° blade pitch angle. More details on polar curve generation and the practical need for optimization can be found in [11]. Based on a similar methodology, new polar curves are optimized to get the proper thrust force on the set point selected for operation. Additional work is currently going on to consolidate the physics behind the optimized polar curves. New polar curves are generated with CFD or tools such as XFoil [9] and AirfoilPrep [10], however the non-standard operating conditions (very low Reynolds number, attack angle beyond the stall) make this work quite complex.

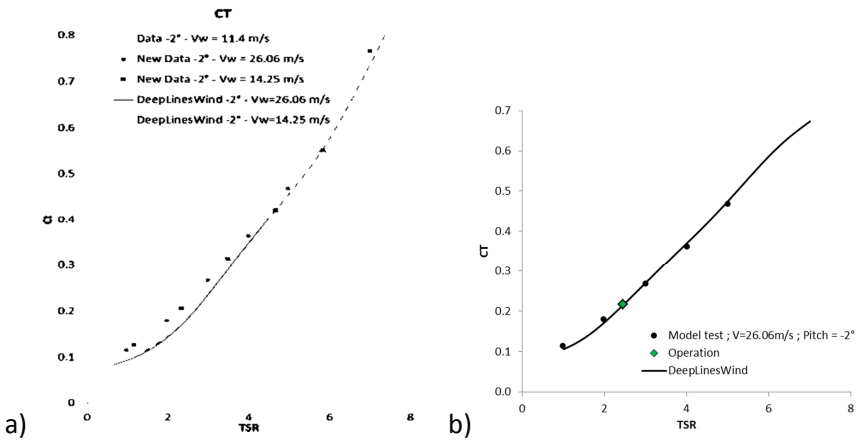

Figure 5-2 : Thrust coefficient versus TSR with a) polar curves from [7] and b) optimized polar curves

The Ct curve obtained with the new polar curves fits quite well the experimental Ct curve in the TSR range of interest (Figure 5-2-b). Based on this solution, a very good match is obtained on the mean values for the forces and moments at the tower top and bottom. To analyze the time variation, power spectral density (PSD) curves are plotted. Whatever the quantity, the trends are quite similar, thus only the x-force at tower top is plotted in Figure 5-3. The

black curve corresponds to the basin measurement, the dark blue to the initial simulation. The following peaks can be identified: a small 1P (P being the rotational frequency) peak around 1.3 rad/s, the most energetic peak associated to tower bending, 3 narrow but high peaks for 3P, 6P and 9P, a broad peak for the blades at very high frequencies.

Various sensitivity analyses are realized, the conclusion being that the wind turbine structure and the wind field should be precisely known and accounted for in order to properly reproduce the spectral content. In Figure 5-3, including the vertical component and time variation of the horizontal wind speed direction (3D wind, red curve) substantially increases the spectrum level. Considering a vertical wind profile, because of the finite size of the wind generator in the basin, generates the 3P peak (green curve). On the opposite, whatever the exact wind speed time series – directly the measured one or one generated with TurbSim based on a Kaimal spectrum and the experimental statistics – the force and moment spectrums remain quite similar. Not represented on the figure, tower shadow activation generates small 3P, 6P and 9P peaks and unbalanced blade mass leads to a small 1P peak.

Some discrepancies with the experimental data still remain. For example, the 6P peak is much higher in the experimental data, a structural frequency missing in the numerical model is probably interacting with the 6P period. This could also explain why this peak is as energetic as the 3P one. For the other signals, the 1P peak is not energetic enough, probably because of a small asymmetry of the rotor or of the drive train. There is also too much energy at low frequencies, the tower peak is too broad. This can be improved by considering a full-field wind (light blue curve), probably closer from reality, instead of the same wind variation all over the rotor. The tower peak shape is improved but then the level of the whole spectrum is too low. This can be corrected by artificially increasing the wind turbulent intensity, then leading to a very good match with the experimental data, however no physical justification can support such a procedure.

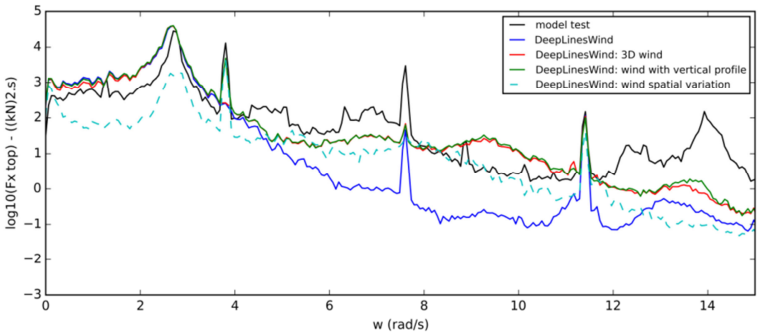

Figure 5-3 : Power spectral density for the x-force at tower top (fixed wind turbine, production case)

To conclude on the aerodynamic aspects, the statistical values (mean value, standard deviation) are quite well predicted by DeepLinesWind whereas some aspects of the spectral content are not. The match has already been improved a lot by accounting for some specificities of the setup.

Investigation is continuing on the fixed wind turbine case before going to the floating tests and to the fully coupled simulations with DeepLinesWind, which will be even more complex in terms of spectral content. Consequently the next paragraph focuses on the floating tests and the comparison with the simplified coupled simulations with Orcaflex.

6. Simplified Coupled Simulation (SCS) results

The results shown below are issued from simplified coupled simulation run with ORCAFLEX. For this type of simulations, the aerodynamics of the wind turbine is not solved by the software, but imposed through force and moment time series measured in the basin at the tower top.

This section shows the comparison between the numerical simulation and the basin test for an extreme operational environment:

- Hs = 6m, Tp = 10s, gamma = 1.3
- Vwind = 26m/s
- No current
- Wave and wind collinear

The model captures in a fairly good manner the statistics measured in the basin. Table 6-1 shows the numerical and experimental statistics of the floater pitch, line tension and tower bottom moment.

Signal	unit	mean		rms		max		min	
		MARIN	ORCAFLEX	MARIN	ORCAFLEX	MARIN	ORCAFLEX	MARIN	ORCAFLEX
Floater pitch	deg	-1.9	-1.7	0.25	0.22	-1.0	-0.9	-2.8	-2.6
Line tension	kN	2625	2650	167	166	3430	3240	2020	2040
Tower Bottom Moment	kNm	42600	43800	3590	3200	60200	61000	19000	29400

Table 6-1: measured and simulated statistics of the floater motions and loads.

On Figure 6-1, the PSD curves for the floater motions and loads are plotted: the numerical model captures very well the overall system behavior observed in the basin.

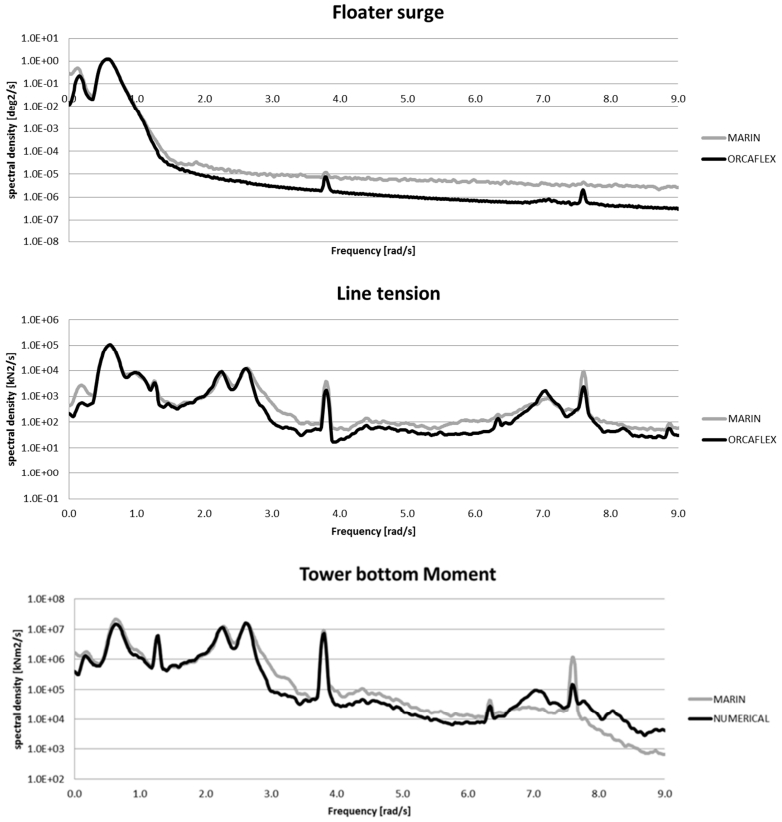

Figure 6-1: PSD, comparison tests vs simulation, a) floater surge, b) most loaded line tension, c) tower bottom moment

A closer look shows that the numerical model slightly underestimates the low-frequency motion around the system natural surge/pitch frequency (~0.13 rad/s). This is still under investigation and several hypotheses are studied (estimation of hydrodynamic coefficients at resonance, wave stretching formulation, …). The impact of this low-frequency component on the design values (maximum motions and tensions and fatigue) is however marginal.

The wave frequency range is very well reproduced by the model for all signals. The mast + lines bending modes (at 2.3 and 2.6 rad/s) are very well captured by the numerical model.

It is important to note that the tower Rayleigh damping coefficient had to be increased to match the tower peak amplitude. This might come from the aerodynamics forcing used in the SCS approach; indeed this aerodynamics signal is not a direct measurement, it is built from a force balance signal from which the inertial part (of the RNA) has been estimated and removed in order to keep only the aerodynamics part. If a small error is made in this correction the signal might inject energy that are not present in the tests and could explain why a higher Rayleigh damping coefficient is required. FCS with DeeplinesWind should remove uncertainties due to aerodynamic forcing.

The above comparisons are performed on an operational case. One can observe the same type of agreement with the parked case simulations: floater motions and loads are also well captured by our numerical models.

7. Conclusion

This paper gives an overview of the different hydrodynamics, aerodynamics and structural checking steps that have been undertaken during the model tests campaign of the IFPEN/SBM floater. The aim of such tests is double: ensuring that the basin setup is well characterized so that the numerical tools can correctly predict the experimental observations, and checking the validity of the hypotheses made during the design phase of a full scale device.

The main outcome of this campaign is the confirmation that the numerical methodology used during the design were able to capture the behavior of the floater. In terms of floater motions, the hydrodynamics tests showed that the floater is weakly sensitive to the hydrodynamics coefficients chosen in the model which could be estimated through DNV-RP-C205, REX and CFD calculation. The analysis of the measured loads (mainly mooring line tension and tower bending moment) highlighted the governing parameters (tower bending stiffness, line stiffness), and once those parameters properly characterized, we show that the numerical simulations give a good agreement with the basin measurements.

The wind turbine and wind setup made available by MARIN, were extensively tested and analyzed thanks to fixed wind turbine tests. They appear to provide appropriate mean loads and spectral content to validate the floater concept, even though some specific aspects of the signal cannot be simulated properly yet. Those aspects, very high 1P and 6P excitations or the precise wind coherence and turbulent intensity, are now believed to be very related to the setup (low Reynolds, structural properties of MSWT, wind field knowledge) and do not question the ability of numerical tools and models.

All the wave tank tests have proved the validity of the inclined-leg TLP concept and have shown a good agreement with the SCS simulations. FCS simulations, with aerodynamic loading computing, is the next step towards the validation of the fully coupled design tools and a better understanding of the concept behavior.

8. References

[1] Melis, C., Bauduin, C., Wattez, A., Newport, A., Poirette, Y., Perdrizet, T., & Averbuch, D. C. (2016, May). Adapting Tension Leg Technology to Provide an Economical Solution for Floating Wind Power. In Offshore Technology Conference. Offshore Technology Conference.

[2] Melis, C., Caille, F., Perdrizet, T., Poirette, Y., Bozonnet, P. (2016). A novel tension-leg application for floating offshore wind: targetting lower nacelle motions. Proceedings of the ASME 2016 35th International Conference on Ocean, Offshore and Arctic Engineering

[3] Le Cunff, C., Heurtier, J. M., Piriou, L., Berhault, C., Perdrizet, T., Teixeira, D., .Gilloteaux, J. C. (2013, June). Fully Coupled Floating Wind Turbine Simulator Based on Nonlinear Finite Element Method: Part I—Methodology. In ASME 2013 32nd International Conference on Ocean, Offshore and Arctic Engineering.

[4] Butterfield, S., Jonkman, J., Musial, W., & Scott, G. (2009). Definition of a 5-MW reference wind turbine for offshore system development. National Renewable Energy Laboratory, Golden, CO, Technical Report No. NREL/TP-500-38060.

[5] De Ridder, E-J., Otto, W., Zondervan, G-J., Huijs, F., Vaz, G. (2014). Development of a Scaled-Down Floating Wind Turbine for Offshore Basin Testing. Proceedings of the 33rd OMAE conference.

[6] DNV, D., & Loads, E. (2010). recommended practice DNV-RP-C205.Environmental conditions and environmental loads. Norway: Det Norske Veritas.

[7] Goupee, A., Kimball, R., de Ridder, E. J., Helder, J., Robertson, A., & Jonkman, J. (2015). A Calibrated Blade-Element/Momentum Theory Aerodynamic Model of the MARIN Stock Wind Turbine. Proceedings of the 25th ISOPE Conference

[8] Jonkman, B. J. (2009). TurbSim user's guide: Version 1.50.

[9] Drela, M. (1989). XFOIL: An analysis and design system for low Reynolds number airfoils. In Low Reynolds number aerodynamics (pp. 1-12). Springer Berlin Heidelberg.

[10] Hansen, C (2012). NWTC Design Codes: AirfoilPrep, http://wind.nrel.gov/designcodes/preprocessors/airfoilprep/.

[11] Gueydon, S., Venet, G., & Fernandes, G. (2015). Influence of the Rotor Characterization on the Motion of a Floating Wind Turbine. In ASME 2015 34th International Conference on Ocean, Offshore and Arctic Engineering.